Penn Libraries
UNIVERSITY of PENNSYLVANIA

University of Pennsylvania
ScholarlyCommons

Departmental Papers (ESE)

Department of Electrical & Systems Engineering

July 2008

Input Impedance, Nanocircuit Loading, and Radiation Tuning of Optical Nanoantennas

Andrea Alù
University of Pennsylvania, andreaal@seas.upenn.edu

Nader Engheta
University of Pennsylvania, engheta@seas.upenn.edu

Follow this and additional works at: http://repository.upenn.edu/ese_papers

Input Impedance, Nanocircuit Loading, and Radiation Tuning of Optical Nanoantennas

Abstract

Here we explore the radiation features of optical nanoantennas, analyzing the concepts of optical input impedance, optical radiation resistance, impedance matching, and loading of plasmonic nanodipoles. We discuss how the concept of antenna impedance may be applied to optical frequencies and how its quantity may be properly defined and evaluated. We exploit these concepts in the optimization of nanoantenna loading by optical nanocircuit elements, extending classic concepts of radio-frequency antenna theory to the visible regime for the proper design and matching of plasmonic nanoantennas.

P H Y S I C A L   R E V I E W   L E T T E R S

Input Impedance, Nanocircuit Loading, and Radiation Tuning of Optical Nanoantennas

Andrea Alù[*] and Nader Engheta[†]

Department of Electrical and Systems Engineering, University of Pennsylvania, Philadelphia, Pennsylvania 19104, USA

Here we explore the radiation features of optical nanoantennas, analyzing the concepts of optical input impedance, optical radiation resistance, impedance matching, and loading of plasmonic nanodipoles. We discuss how the concept of antenna impedance may be applied to optical frequencies and how its quantity may be properly defined and evaluated. We exploit these concepts in the optimization of nanoantenna loading by optical nanocircuit elements, extending classic concepts of radio-frequency antenna theory to the visible regime for the proper design and matching of plasmonic nanoantennas.

The research in optical plasmonic materials, fostered by remarkable advancements in nanotechnology, is currently leading towards the realization of integrated plasmonic devices that may have functionalities similar to their radio-frequency (RF) counterparts but with much enhanced bandwidth, speed, and compactness. Driven by these advancements, and, in particular, by the possibility of realizing plasmonic nanorods with elongated shapes and relatively high aspect ratios, several groups have experimentally investigated the realization of nanoantennas in the form of monopole and dipole antennas made of plasmonic materials [1–6]. From a theoretical point of view, however, the recipe for proper design and performance optimization of these nanoradiators is still in its embryonic stage when compared with well-known design methods for conventional RF transmitting antennas. A recent Letter [7] has pointed out the shortening of the effective wavelength of a guided mode traveling along a plasmonic dipole with respect to the free-space wavelength, consistent with the well-known slow-wave properties of plasmonic nanorods [8]. All such studies, however, have been concerned with the scattering properties of these components when illuminated by external sources, e.g., light beams or microscope tips, or with their interaction with nanostructures nearby. It is interesting to note, on the other hand, that by definition the main functions of any antenna include ''connecting'' and ''matching'' a source, a receiver, or a waveguide to the ''outside'' region (e.g., free-space domain) in order to transmit (or receive) a given signal to (or from) the far field. In this sense, the concepts of input impedance at the feeding point, the antenna's radiation resistance, and the role of loading an antenna, all of which are familiar notions for traditional RF antennas, are quantities of fundamental importance for a proper design and use of antennas. These parameters, however, cannot be obtained from the scattering analysis and necessitate a proper definition at IR and optical frequencies, where the dispersion of metals cannot be ignored and metals do not possess high conductivity. Inspired by the RF antenna concepts, here we develop the concepts of optical input impedance, optical radiation resistance, loading, and impedance matching in the optical domain, and we investigate them for plasmonic nanoantennas in the form of nanodipoles, with the goal of bringing some of the RF designs into nano-optics. We have theoretically utilized these concepts to tailor and shift at will the scattering resonance of optical nanoantennas in Ref. [9].

The geometry of the problem is depicted in Fig. 1, which consists of a cylindrical nanodipole of total length L and radius R, made of silver and terminated on both sides by spherical tips. The dipole is assumed to be fed at its center gap of thickness g. This resembles a conventional center-fed RF dipole antenna; however, here the optical nanoantenna is made of silver, a low-loss noble metal whose permittivity at the frequencies of interest is well described by a classic Drude model $\varepsilon_{Ag} = \varepsilon_0\{\varepsilon_\infty - f_p^2/[f(f + i\gamma)]\}$, with $\varepsilon_\infty = 5$, $f_p = 2.175$ PHz, and $\gamma = 4.35$ THz [10].

Feeding the nanoantenna at its gap allows one to determine its optical input impedance $Z_{in} = R_{in} - iX_{in}$, which is defined here as the ratio of the driving optical voltage difference across the gap to the total flux of induced optical displacement current flowing from the feeding source into the antenna (and the gap). This is quite distinct from a
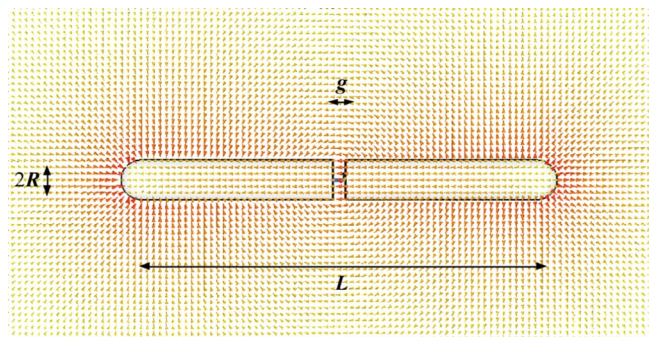

FIG. 1 (color online). Geometry and electric field distribution in the E plane (snapshot in time) at the resonant frequency for which $L \simeq \lambda_{eff}/2$ for a silver nanodipole antenna. In this case, $L = 110$ nm and $f = 266$ THz. Brighter colors and longer arrows correspond to larger field levels.

classic dipole antenna at low frequencies, for which the current defining the input impedance is given by the conduction current flowing on the surface of the antenna made of highly conductive metal. Here, due to the lack of conductivity in optical materials, these concepts need to be properly reconsidered and redefined. Figures 2(a) and 2(b) report R_{in} (resistive component) and X_{in} (reactive component) for different lengths of the nanodipole, while $R = 5$ nm and $g = 3$ nm kept fixed, using full-wave time-domain simulation software [11]. For very low frequencies, the silver is a conductive metal, and the corresponding impedance is strongly capacitive (i.e., $X_{in} < 0$), analogous to a short RF dipole. However, by increasing the frequency up to the IR and visible regime, the plasmonic features of silver come into play, and the antenna hits its first resonance at the frequency for which $X_{in} = 0$, indicated, as an example, by the blue arrow in Fig. 2(b) for the $L = 160$ nm curve, i.e., at a lower frequency compared with a conducting dipole of the same length. It is evident that, by decreasing the length L, the antenna resonant frequency shifts up, analogous to the case of a regular RF dipole. Its position is located around the frequency for which the condition $L =$
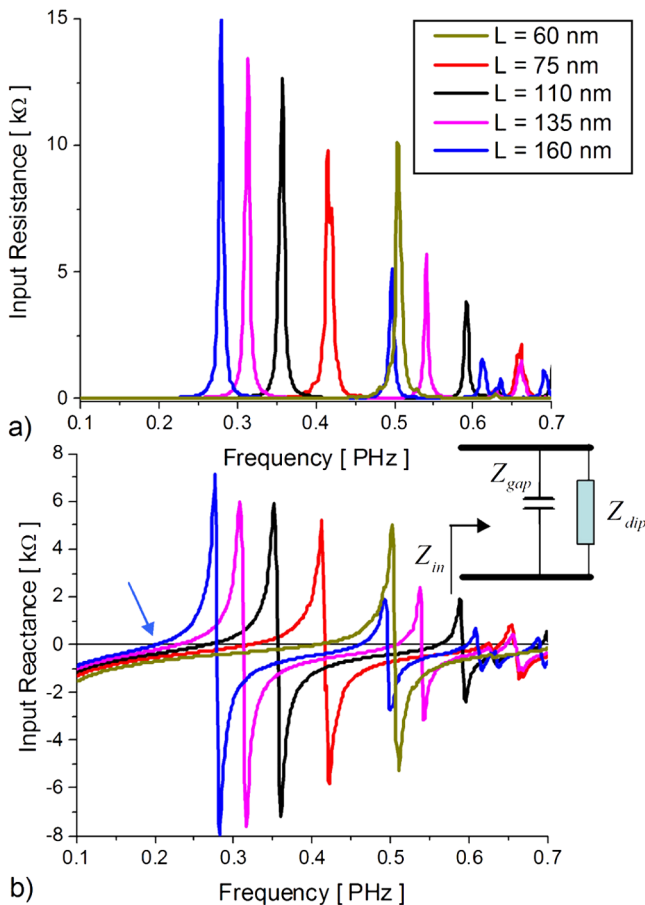

a)

b)

FIG. 2 (color online). (a) Input resistance (R_{in}) and (b) input reactance (X_{in}) for the dipole nanoantenna of Fig. 1 made of silver, with $R = 5$ nm and $g = 3$ nm varying L.

$\lambda_{eff}/2$ holds, where λ_{eff} is the effective wavelength experienced by the plasmonic dipole, which is shorter than the free-space wavelength λ_0 [7]. The value of the input resistance at this resonance frequency is lower than that of a regular RF dipole antenna (for instance, $R_{in} = 22.2 \ \Omega$ for the dipole of Fig. 1 with $L = 110$ nm), as discussed in the following. Consistent with the transmission-line model of a dipole [12], this first resonance has a low input impedance, and it may be seen as a "short-circuit" resonance (i.e., $X_{in} = 0$) associated with the condition $L = \lambda_{eff}/2$. In contrast, a sharp "open-circuit" resonance (i.e., where R_{in} and X_{in} are very large) is also noticed in Fig. 2 at a somewhat higher frequency, which corresponds to the sharp impedance resonance in the plots. The impedance values associated with this resonance here are larger than those obtained at the $L = \lambda_0$ resonance for a regular conducting RF dipole antenna with a similar aspect ratio, owing to the plasmonic properties of the nanoantenna, which introduce higher confinement of the stored fields and non-negligible Ohmic losses, both increasing the value of the input impedance. Moreover, the open-circuit resonant frequency is lower than the $L = \lambda_{eff}$ frequency, due to the non-negligible capacitance of the air gap region in this geometry, which is required for a proper loading of the dipole as discussed in the following. The input impedance evaluated in Fig. 2 may indeed be regarded as the parallel combination of the "intrinsic" impedance of the nanodipole Z_{dip} and the air gap capacitive impedance Z_{gap}, consistent with the circuit model in the inset in Fig. 2(b). This second resonance therefore arises when the inductive reactance of the nanodipole itself (at a frequency higher than the short-circuit resonance) resonates with the air gap capacitance, resulting in large input impedance. This open-circuit resonance actually coincides with the scattering resonant frequency [9].

A regular RF radiating antenna is usually operated at the short-circuit resonance for matching reasons, but for the optical nanoantenna operation both of these resonant frequencies may be appealing, depending on the impedance of the feeding mechanism (the peak values of input resistance and reactance in Fig. 2 around the open-circuit resonance may be comparable with the characteristic impedance of subdiffractive plasmonic waveguides [13]).

In Fig. 1 of the supplementary material [14(a)], we have plotted the optical nanoantenna efficiency η_{eff}, known as the ratio between the total radiated power P_{rad} and the power effectively "accepted" into the antenna input terminals. Although the peak of efficiency is located near the open-circuit resonance, the optical radiation efficiency is reasonably high over a wide frequency window around $L = \lambda_{eff}/2$, despite the material loss in silver and the nanodipole plasmonic features.

Figure 1 reports the electric field distribution in the E plane for a nanodipole with $L = 110$ nm at the short-circuit frequency $f = 266$ THz (at this frequency

$\lambda_{\mathrm{eff}} \simeq 255$ nm, slightly larger than the resonance condition $\lambda_{\mathrm{eff}} = 2L$, due to the reactive fields at the end of the dipole, which may be approximately taken into account by introducing an effective dipole length $L_{\mathrm{eff}} \simeq L + 2R$, consistent with Ref. [7]). The field distribution resembles that of a conventional half-wavelength resonant RF dipole, ensuring reasonably good radiation and matching at the input port. However, we note the peculiar longitudinal electric field distribution inside the silver dipole, responsible for the flow of optical displacement current along the antenna, drastically different from a classic dipole antenna. This current effectively plays the role of the conduction current flowing on the surface of an RF dipole made of highly conductive material.

Analogous to the case of RF antennas, for the plasmonic optical nanodipole here we may define an optical radiation resistance as $R_{\mathrm{rad}} = 2P_{\mathrm{rad}}/I_{\max}^2$, with $I_{\max}$ being the peak of current along the dipole. However, following the previous discussion and the concepts of optical nanocircuits [15,16], the current flow along the nanodipole should consider now the flux of optical displacement current, denoted as $-i\omega\varepsilon_{Ag}E_0$, with E_0 being the local electric field in silver. In the limit of thin nanodipoles (i.e., $R \ll L$), an approximate standing wave displacement current distribution is expected along the dipole, with expression $I(z) = I_0 \sin[\pi(L_{\mathrm{eff}} - 2|z|)/\lambda_{\mathrm{eff}}]/\sin[\pi L_{\mathrm{eff}}/\lambda_{\mathrm{eff}}]$, with I_0 being the current entering the nanoantenna arms at the feeding point [17]. The corresponding optical radiation resistance may be evaluated in closed form (not reported here, for its length, but plotted in Fig. 2 of the supplementary material [14(b)]).

The predicted values of resistance are lower, but comparable in magnitude, than those expected from an RF dipole. This effect is due to the shortening of λ_{eff} (compared with λ_0), which leads to an electrically smaller radiation aperture as compared with analogous classic RF dipoles. At the frequency for which $L_{\mathrm{eff}} = \lambda_{\mathrm{eff}}/2$ (which corresponds to the thin solid line in Fig. 2 of the supplementary material [14(b)]), $I_{\max} = I_0$, implying that the value of radiation resistance is "seen" at the input port. Because of the material losses in the nanoantenna, this value is somewhat lower, but comparable in magnitude, than the input resistance at the short-circuit resonant frequency, validating and explaining our numerical results for the radiation efficiency [14(b)]. The radiation efficiency may, in general, be given by $\eta_{\mathrm{eff}} = \frac{R_{\mathrm{rad}}}{R_{\mathrm{rad}} + \sin^2(\pi L_{\mathrm{eff}}/\lambda_{\mathrm{eff}})R_{\mathrm{loss}}} = \frac{R_{\mathrm{rad}}}{\sin^2(\pi L_{\mathrm{eff}}/\lambda_{\mathrm{eff}})R_{\mathrm{in}}}$, where R_{loss} is the portion of input resistance associated with the power lost through absorption in the silver. R_{rad} increases for longer antennas, as seen in Fig. 2 of the supplementary material [14(b)], since longer nanodipoles resonate at lower frequencies, for which the effect of wavelength shortening is reduced. This is consistent with the corresponding increase in η_{eff} [14(a)].

The above analysis of the nanodipole input impedance allows treating the two arms of an optical nanoantenna as

the "terminals" of a "lumped" element, which in turn would facilitate the design of a feeding optical waveguide, analogous to what is commonly practiced in conventional RF dipole antenna design. This suggests the possibility of designing suitable "nanoloads" for this optical antenna using optical lumped circuit elements [15] in order to adjust and tune the nanodipole resonant frequency or to "match" the nanoantenna with a feeding network at nanoscales. To this end, we "load" the nanodipole of Fig. 1 at its gap region with a nanoparticle (e.g., a nanodisk) made of a material with permittivity $\varepsilon_{\mathrm{load}}$ that acts as an optical lumped element [i.e., a nanocapacitor (nanoinductor) when $\mathrm{Re}(\varepsilon_{\mathrm{load}})$ is positive (negative)]. In this scenario, the load effectively replaces the air gap and becomes in "parallel" with the antenna terminals, which can still be fed at the gap, for instance, by a plasmonic waveguide, as sketched in the inset in Fig. 3(b) together with the modified circuit model.
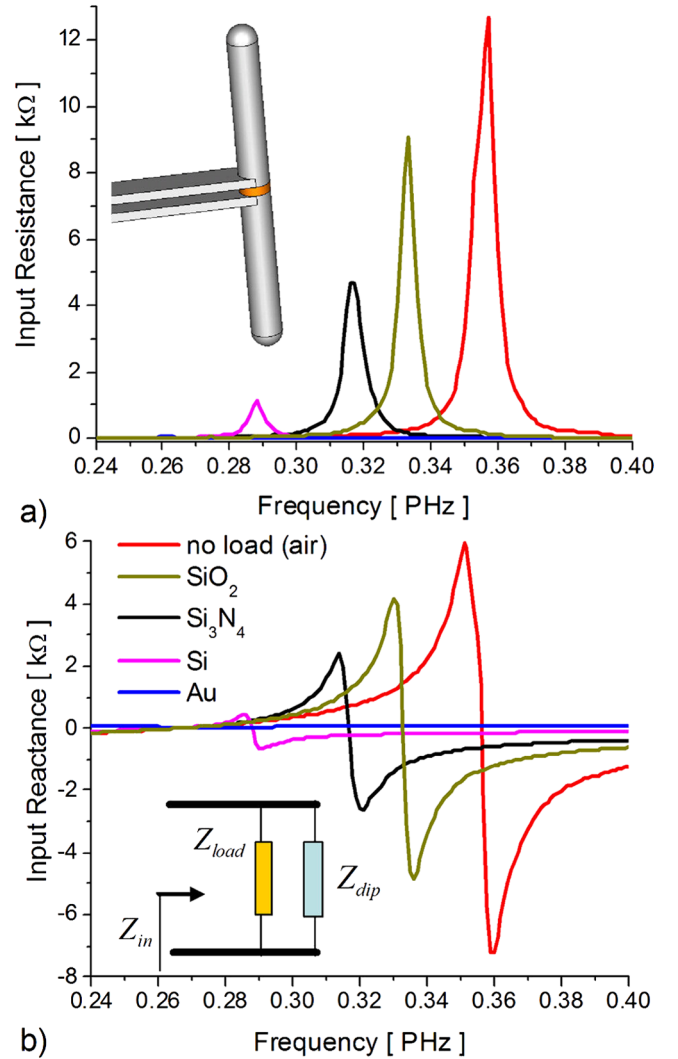

FIG. 3 (color online).   (a) Input resistance and (b) input reactance for the loaded nanodipole antenna of Fig. 1 with $L = 110$ nm, varying the material of nanoload at its gap.

Figure 3 reports the modification of the input resistance and reactance of the nanodipole, after being loaded with nanodisks of different permittivity. It is evident how the open-circuit resonant frequency may be tuned to the desired value by properly choosing the nanocapacitance or nanoinductance at the gap terminals, without changing the nanodipole length. We point out that this shift in the resonant frequency is not only predictable *qualitatively*, but it is indeed *quantified* and *tailored* at will, similar to the antenna design at RF, by applying the concepts introduced in this Letter. Following our optical nanocircuit theory [15], the load impedance may indeed be easily evaluated as $Z_{load} = ig/(\omega \varepsilon_{load} \pi R^2)$, being capacitive (inductive) for positive (negative) $\mathrm{Re}(\varepsilon_{load})$.

Since the nanoload is replacing the air gap, it is not surprising to discover that the open-circuit resonant frequency, as obtained in Fig. 3, *quantitatively* coincides with the frequency for which the value of the parallel load reactance $X_{load} = -\mathrm{Im}(Z_{load})$ resonates with the dipole's intrinsic reactance $X_{dip} = -\mathrm{Im}[Z_{dip}]$ after proper deembedding or removing the effect of the air gap impedance Z_{gap}. The different curves in Fig. 3 may indeed be obtained with excellent agreement by considering the parallel combination of the input impedance of Fig. 2 with a capacitance represented by the "additional" parallel load $Z_{add} = (Z_{load}^{-1} - Z_{gap}^{-1})^{-1} = ig/[\omega(\varepsilon_{load} - \varepsilon_0)\pi R^2]$. For instance, when a Si_3N_4 nanoload is used in place of the air gap, as seen in Fig. 3, the open-circuit resonance is shifted to 317 THz, at which $X_{in} = 700\ \Omega$ from Fig. 2(b), and this is equal to $\mathrm{Im}[Z_{add}]$. Similar considerations may be verified for the other loads considered in Fig. 3.

Since a larger value of permittivity introduces a larger capacitance for the nanoload, the open-circuit resonance shifts to a lower frequency. By contrast, using a nanodisk made of materials with $\mathrm{Re}(\varepsilon_{load}) < 0$ (i.e., an inductive load), as it was done by considering a gold nanodisk [blue curve in Fig. 3(b)], shifts the resonant frequency downward to a value below the short-circuit frequency in the region where $X_{dip} < 0$. The short-circuit resonance is not modified by the presence of a parallel nanoload, since this resonance is due to the nulling of the intrinsic reactance of the nanodipole without the gap impedance. This resonance may, however, be tuned using a *series* nanoload, placed between the feeding terminals and the antenna arms (not shown here).

The above discussion effectively shows that the concept of nanoantenna loading will become analogous to its RF counterpart, if the optical nanocircuit elements [9,15,16] are used to quantify the load impedance as suggested here. An interesting corollary to this observation is that the input resistance at resonance is consistently reduced, when the permittivity of the parallel nanodisk load is increased [see Fig. 3(a)], again fully consistent with the circuit model that we have introduced. A judicious design of the parallel loads may allow a good matching between the nanodipole

antenna and its feeding system at the open-circuit resonance (e.g., a plasmonic waveguide). These results may facilitate the tuning and use of these nanoantennas for various applications in optical communications, biological and medical sensors at the nanoscales, and nano-optical microscopy.

---

*andreaal@ee.upenn.edu

†To whom correspondence should be addressed. engheta@ee.upenn.edu

[1] K. B. Crozier, A. Sundaramurthy, G. S. Kino, and C. F. Quate, J. Appl. Phys. **94,** 4632 (2003).

[2] P. J. Schuck, D. P. Fromm, A. Sundaramurthy, G. S. Kino, and W. E. Moerner, Phys. Rev. Lett. **94,** 017402 (2005).

[3] P. Muhlschlegel, H. J. Eisler, O. J. F. Martin, B. Hecht, and D. W. Pohl, Science **308,** 1607 (2005).

[4] J. Aizpurua, G. W. Bryant, L. J. Richter, F. J. García de Abajo, B. K. Kelley, and T. Mallouk, Phys. Rev. B **71,** 235420 (2005).

[5] E. Cubukcu, E. A. Kort, K. B. Crozier, and F. Capasso, Appl. Phys. Lett. **89,** 093120 (2006).

[6] E. K. Payne, K. L. Shuford, S. Park, G. C. Schatz, and C. A. Mirkin, J. Phys. Chem. B **110,** 2150 (2006).

[7] L. Novotny, Phys. Rev. Lett. **98,** 266802 (2007).

[8] J. Takahara, S. Yamagishi, H. Taki, A. Morimoto, and T. Kobayashi, Opt. Lett. **22,** 475 (1997).

[9] A. Alù and N. Engheta, Nat. Photon. **2,** 307 (2008).

[10] P. B. Johnson and R. W. Christy, Phys. Rev. B **6,** 4370 (1972).

[11] We have used CST STUDIO Suite 2006B, http://www.cst.com. The features of this geometry have been analyzed with a 0.2 nm detail with suitable subgridded discretization and proper full convergence has been ensured to a −80 dB level.

[12] C. A. Balanis, *Antenna Theory* (Wiley, New York, 1996).

[13] A. Alù and N. Engheta, J. Opt. Soc. Am. B **23,** 571 (2006).

[14] (a) See EPAPS Document No. E-PRLTAO-101-059830. (a) Figure 1 in the Supplementary Material. Radiation efficiency, related to Fig. 2. In order to increase the numerical precision, each one of these curves has been obtained with frequency-domain simulations (310 frequency samples all over the frequency range of the figure). (b) Figure 2 in the Supplementary Material. Radiation resistance for the nanodipoles of Fig. 2. The thinner solid line indicates the theoretical radiation resistance evaluated for a nanodipole with $L_{eff} = \lambda_{eff}/2$ (at RF this line would be constant at 73 Ω). For more information on EPAPS, see http://www.aip.org/pubservs/epaps.html.

[15] N. Engheta, A. Salandrino, and A. Alù, Phys. Rev. Lett. **95,** 095504 (2005).

[16] N. Engheta, Science **317,** 1698 (2007).

[17] This expression considers the flow of displacement current at the tips of the nanodipole by using the effective dipole length $L_{eff} \simeq L + 2R$. Contrary to a conventional RF dipole, here the current at the physical tip of the nanodipole is not necessarily zero, since we are considering the displacement current as the flowing current in the system.